Indian Journal of Pure & Applied Physics
Vol. 61, May 2023, pp. 355-365
DOI: 10.56042/ijpap.v61i5.69090

Noise Analysis of Grover's Quantum Search Algorithm

Tarun Kumar[a], Dilip Kumar[a] & Gurmohan Singh[b*]

[a]Department of Electronics and Communication Engineering, SLIET, Longowal, Punjab 148 106, India

[b]Centre for Development of Advanced Computing (C-DAC), Mohali, Punjab 160 071, India

Received 26 November 2022; accepted 18 April 2023

For searching an item in unstructured databases, Grover's quantum search algorithm offers quadratic speedup over classical search algorithms. This paper reports 2 to 5 quantum-bit (Qubit) implementations of Grover's search algorithm using the phase-flip method for oracle function realization without any extra ancilla qubit. A comprehensive estimation and analysis of the theoretical and physical accuracies of the algorithm have been presented. The impact of increasing qubits on accuracy has been computed and analyzed. The metrics delineated for comparison are the number of qubits and gates, depth of the circuit, execution time, and theoretical/physical accuracy. The results revealed a greater disparity between theoretical and physical accuracy using a higher number of qubits perceived to be caused by noisy qubits utilized in computations. The novelty of the work is the investigation of variations caused by the noise in the accuracy and execution time of Grover's search algorithm. The results indicate that because of noise, the accuracy of 2- and 3- qubit implementations declined by 14.49% and 33.86%, whereas the execution time increased by 50% and 80%; respectively.

Keywords: Grover's algorithm; Initialization; Oracle; Amplitude amplification; CNOT; Qubit; Phase-flip; Noise

1 Introduction

Quantum computers promise significant improvement in terms of speedup for some specific set of hard computational problems intractable with classical counterparts[1]. Nowadays, data is growing bigger at a much faster rate which leads to the problem of handling and subsequently processing bigger datasets[2]. In order to search for a particular item in a big unstructured dataset, classical search algorithms face difficulties[3] and get very intricate as the data is in the form of matrices and vectors. To overcome this problem, quantum search algorithms promise superior performance. In quantum computing, algorithms are based on linear algebra with data encoded in the form of matrices and vectors, so they can handle big datasets more efficiently, which leads to the improved speed of desired operation[4-6]. Quantum algorithms like HHL algorithm[7] for matrix inversion, Shor's algorithm[8] for factoring large numbers into primes providing exponential speedup, and Grover's algorithm[9] for searching an item in an unstructured database promise quadratic speedup.

Quantum computer operates by controlling the behaviour of sub-atomic particles based on principles of superposition and entanglement[10-11]. The basic unit of information in quantum computation is Quantum-bit (Qubit) which is a unit vector in 2-dimensional vector space and represented by basis vectors $|0\rangle$ or $|1\rangle$. Basis vector $|0\rangle$ corresponds to $|\uparrow\rangle$ polarization of a photon or an electron's spin-up position and $|1\rangle$ corresponds to $|\downarrow\rangle$ polarization of a photon or electron's spin-down position[10]. Classical bits' *'0'* and *'1'* can be represented by basis vectors $|0\rangle$ and $|1\rangle$ in quantum computing[10, 12]. A single qubit stores *'0'* and *'1'* simultaneously, whereas a 2-qubit system can be in four states, i.e., *'00', '01', '10'*, and *'11'* simultaneously. Quantum computers work like probabilistic as well as non-deterministic computers[13].

Although a qubit can be in an infinite number of super positions, it can only draw out information equivalent to a classical bit. It happens because of the measurement. When the measurement is applied to a qubit, it changes its state to any of the basis states. After measurement in $\{|0\rangle, |1\rangle\}$ basis, quantum computers produce results in any of the two states when it is in an equal superposition of $|0\rangle$ and $|1\rangle$[13-14]. Quantum gates are the circuits that perform manipulations on qubits. The basic gates in quantum computing are Hadamard gate utilized to create superposition, Pauli gates (X, Y and Z) are single-qubit used for representing rotation operation about x, y and z axes of the Bloch sphere by π radians, and Controlled NOT (CNOT/CX) gate to produce entanglement operation[12-15].

*Corresponding author: (E-mail: gurmohan@cdac.in)

This paper reports a comparison of the theoretical accuracy of Grover's algorithm with the physical accuracy. The theoretical accuracy is computed using a simulator[16], while physical accuracy is computed using a real-time quantum computer[17]. The 2-to-5 qubit implementations of Grover's algorithm are considered for comparison[3,18-21] for different number of iterations. The variations in the accuracy and execution time caused by noise present in real-time quantum computers is also investigated for 2-to-5 qubit implementations of Grover's algorithm.

The structure of this paper is as follows: Section 2 introduces a brief introduction to quantum algorithms and describes Grover's algorithm in detail. Section 3 enumerates the various implementations of Grover's algorithm. Section 4 presents the experimental evaluation and comparison of various implementations of Grover's algorithm. Section 5 presents the noise analysis of Grover's algorithm up to 5-qubit implementations. Section 6 outlines the conclusion of the paper.

2 Quantum Algorithms

There are numerous algorithms designed for specific problems in classical as well as quantum computing. Some quantum algorithms offer non-exponential speedup than classical algorithms[14] e.g. Grover's algorithm[9]exploited to search an unstructured database and provide a quadratic speedup ($O\sqrt{N}$).Some quantum algorithms promise exponential speedup e.g.Simon's algorithm to find the periodicity of any function[22]and Shor's factoring algorithm for factoring integers[8].

2.1 Grover's Algorithm

Grover's algorithm is developed by L.K. Grover in 1996 for searching an item[9] in an unstructured database of N items, as shown in Fig 1. Classical algorithms perform searching for a particular item in $O(N)$ operations, whereas Grover's algorithm performs the same task in $O(\sqrt{N})$ operations[23]. Hence, this algorithm delivers quadratic speedup over classical counterparts. This unstructured database has 2^n states, i.e., $N = 2^n$, where n is the number of qubits and N is the size of the database[24-25].

In order to find a particular item (say purple item) in the unstructured database of N items, this item is called *winner* and denoted by w. The purple item is referred to as marked item, whereas the rest of the items in the database are unmarked items. There are four stages of applying Grover's algorithm- initialization, oracle formation, amplitude amplification, and measurement. An equal superposition of all states is generated in the initialization step. The oracle formation and amplitude amplification are major steps in this algorithm. The output is measured in the final step.

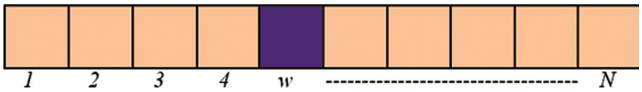

Fig. 1 — Querying an item in an unstructured database.

Oracle is just like a black box that has theability to recognize the solutions to a search problem[26]. Oracle is applied as described in (1) as

$$f(x) = \begin{cases} 0, for\ all\ the\ unmarked\ items \\ 1, for\ marked\ item\ (winner) \\ \quad such\ that\ x = w \end{cases} \quad ...(1)$$

This function *f(x)* is encoded into a unitary matrix such that x, w ϵ $\{0, 1\}^n$ and oracle matrix[4] acting on the standard basis states $|x\rangle$is given by (2) as

$$U_w|x\rangle = (-1)^{f(x)}|x\rangle \quad ...(2)$$

The oracle transformation matrix U_w is represented as (3)

$$U_w = I - 2|w\rangle\langle w| \quad ...(3)$$

where I is the identity matrix,$|w\rangle$ is the solution for the given search problem and $|w\rangle\langle w|$ is the outer product of $|w\rangle$with itself.

If $|x\rangle = |w\rangle$ then

$$U_w|w\rangle = I|w\rangle - 2|w\rangle\langle w|w\rangle = I|w\rangle - 2|w\rangle = -|w\rangle \ldots(4)$$

If $|x\rangle \neq |w\rangle$ then

$$U_w|x\rangle = I|x\rangle - 2|w\rangle\langle w|x\rangle = I|x\rangle = |x\rangle \quad ...(5)$$

Oracle inverts the marked item, whereas it keeps the unmarked items unchanged. This oracle is a diagonal matrix where the marked item will have a negative phase. The matrix is given by (6) as

$$U_w = \begin{bmatrix} (-1)^{f(0)} & 0 \ldots & 0 \\ 0 & (-1)^{f(1)} \ldots & 0 \\ : & :: & : \\ 0 & 0 \ldots & (-1)^{f(2^n)} \end{bmatrix} \quad ...(6)$$

The amplitude of the marked item is stretched out, whereas the amplitude of unmarked items is lowered when Grover's diffusion operator is applied[27]. Measuring the final state yields the marked item with high certainty. Grover's diffusion operator[3] for the amplitude amplification or inversion about the mean of the target item is given by (7) as

$$U_s = 2|s\rangle\langle s| - I \quad ...(7)$$

where $|s\rangle$ is the superposition of the states, and I is the Identity matrix. The diffusion matrix (U_S)is

$$\begin{bmatrix} \frac{2}{N}-1 & \frac{2}{N} & \dots & \frac{2}{N} \\ \frac{2}{N} & \frac{2}{N}-1 & \dots & \frac{2}{N} \\ \vdots & \vdots & \vdots & \vdots \\ \frac{2}{N} & \frac{2}{N} & \dots & \frac{2}{N}-1 \end{bmatrix}$$

The implementation steps for Grover's algorithm are illustrated below:

(i) Prepare $|0\rangle^{\otimes n}$ where $|0\rangle^{\otimes n}$ means $|0\rangle\otimes|0\rangle\otimes\dots\dots\dots\otimes|0\rangle$ for n times and $\otimes$ means tensor product[3]. Then, create the superposition of 2^n states. The superposition is created by applying the Hadamard gate on $|0\rangle^{\otimes n}$i.e.$H^{\otimes n}|0\rangle^{\otimes n}$ as described by (8)

$$|s\rangle = (H|0\rangle)^{\otimes n} = \frac{1}{\sqrt{N}}\sum_{x=0}^{N-1}|x\rangle \quad \dots(8)$$

where, $|s\rangle$ is the superposition of all the states and $\frac{1}{\sqrt{N}}$is the amplitude[10].

Fig. 2(a) illustrates the initial state as a geometric representation of two perpendicular vectors in two-dimensional space, whereas Fig. 2 (b) represents the amplitude of the |s⟩ state for N items in the form of bar graph.

(ii) Apply oracle on $H^{\otimes n}|0\rangle^{\otimes n}$ to reflect the target item[12]. Define a function $f:\{0,\dots\dots,N-1\}\rightarrow\{0,1\}$is defined as (9)

$$f(x) = \begin{cases} 1, if\ x\ is\ searched \\ 0, Otherwise \end{cases} \quad \dots(9)$$

where x is the target item. Oracle is applied such that[18, 13]

$$U_w|x\rangle = (-1)^{f(x)}|x\rangle \quad \dots(10)$$

Figure 3(a) geometrically represents the reflection of superposition state |s⟩ to $U_w|s\rangle$ when oracle is applied. Fig. 3(b) represents the amplitude negation of the marked state |w⟩ while keeping the unmarked states unaffected, as described by equations (4) and (5).

(iii) Now apply Grover's diffusion operator (U_s) for the amplitude amplification or inversion about the mean of the target item[26]. This operator can be applied by using phase shift gate[21]. This transformation maps the state to $U_sU_w|s\rangle$ and completes the transformation[4].

The diffusion operator applied to the state $U_w|s\rangle$ results in additional reflection and maps $U_w|s\rangle$ to $U_sU_w|s\rangle$ geometrically. The reflection of the state $U_w|s\rangle$ occurs about the state |s′⟩ as shown in Fig. 4(a). Fig. 4 (b) reveals that the amplitude of the marked state |w⟩ is inverted and amplified when the diffusion operator is applied, whereas the amplitude of the unmarked states is lowered.

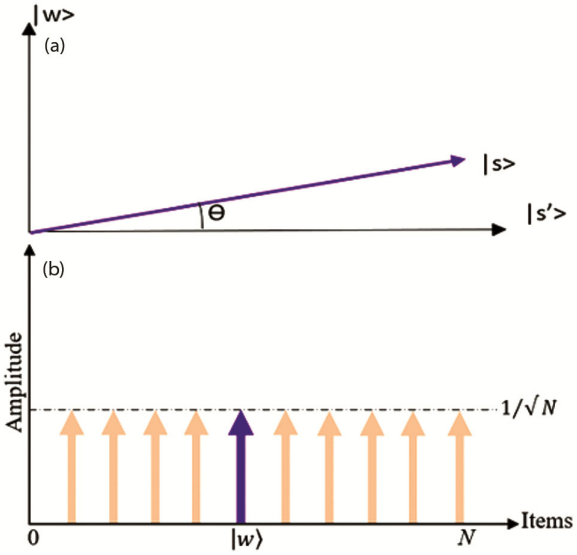

Fig. 2 — (a) is the geometric representation of two perpendicular vectors |s′⟩ and |w⟩ in two-dimensional space which expresses the initial state as |s⟩ = sinθ|w⟩+cosθ|s′⟩, where, θ= arcsine (1/√N), and (b)Amplitude of the |s⟩ state for N items in the form of bar graph[28].

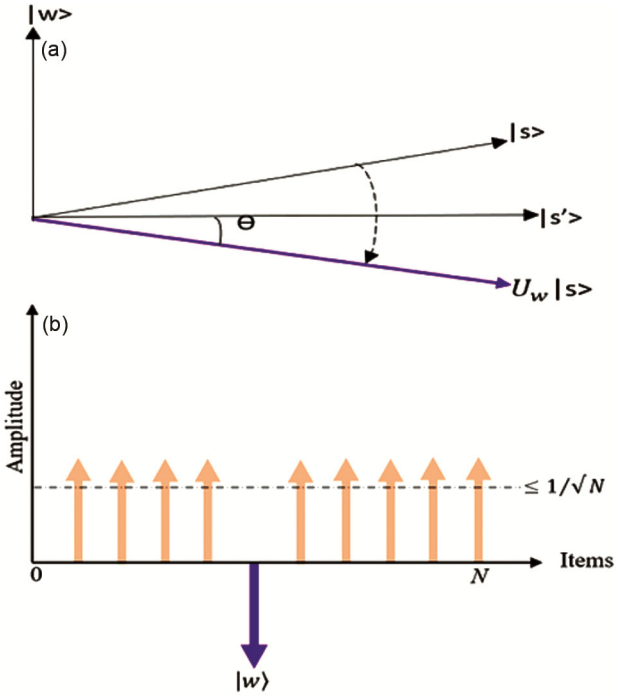

Fig. 3 — (a) Corresponds to a reflection of the state |s⟩ to $U_w|s\rangle$ about |s′⟩ geometrically, and (b) shows that the amplitude of marked state |w⟩ becomes negative and the average amplitude is lowered[28].

(iv) Repeat steps *(ii)* and *(iii)* $O(\sqrt{N})$ times, i.e., $k = round\left(\frac{\pi}{4}\sqrt{N}\right)$.

(v) Measure the output[10, 18].

Figure 5 reveals the schematic circuit of Grover's search algorithm for a database of size *N*. The size of the database is equal to the number of states, i.e., $N = 2^n$. Qubits are initialized and put into superposition by using the Hadamard gate. Oracle (U_w) followed by the Grover diffusion operator is used to search the correct marked state and repeated $O(\sqrt{N})$ times. Measurement is taken in the end to detect the correct marked state.

3 Implementation of Grover's Algorithm

The encoding methods which can be used for state marking in the oracle are boolean and phase flip methods. The Boolean method uses the NOT and $C^k(NOT)(k \leq n)$gates to construct oracles where $C^k(NOT)$ is targeted on the ancilla qubit (initialized to $|1\rangle$), which flips the phase of the marked state.

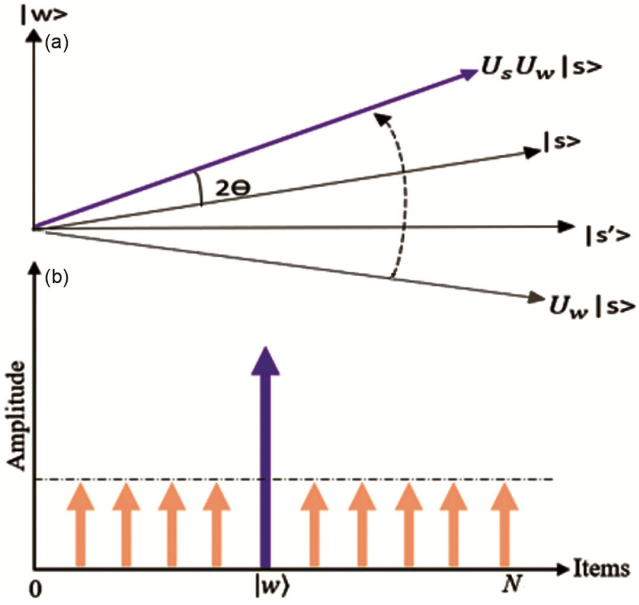

Fig. 4 — (a) Corresponds to a reflection of the state $U_w|s\rangle$ to $U_sU_w|s\rangle$ about $|s'\rangle$ geometrically, and (b) shows the increased amplitude of state $|w\rangle$[28].

The phase flip method uses Z and $C^k(Z)$ gates to build oracles and flips the phase of the marked state directly. The phase flip method is used for the construction of oracle in all implementations reported in this paper instead of the boolean method, as the latter requires ancilla qubits and other resources. The algorithm executes states $|11\rangle$, $|111\rangle$, $|1111\rangle$, and $|11111\rangle$. Quantum gates such as Hadamard, Pauli-(X, Z), controlled-Z, multi-controlled Z, C-NOT, Toffoli gate (CCX), and multi-controlled-NOT gates are used for the different implementations of Grover's algorithm. The circuit diagrams with a brief description of Grover's algorithm for 2-, 3-, 4-, and 5-qubit are provided. All the implementations are done using a different number of iterations. Grover's algorithm with 2-qubit, 3-qubit, and 4-qubit is implemented with single, up to two, and up to three iterations, respectively. This paper includes the implementation of Grover's algorithm for 5-qubit with up to four iterations, which is not demonstrated earlier. The circuit diagrams in Figs. 6 - 9 are divided into four parts which include (a) initialization, (b) oracle formation, (c) diffusion operator or amplitude amplification, and (d) measurement.

3.1 Five Qubit Implementation

The 5-qubit implementation of Grover's algorithm for a single iteration divided into four steps is briefly illustrated. Phase flip technique for the construction of oracle and diffusion operator is used. In the 5-qubit implementation, the initialization step puts qubit $|q_0\rangle$ to $|q_4\rangle$ in the superposition. The superposition of qubits is achieved by using the Hadamard gate on all the qubits, as shown in Fig. 9(a). The amplitude of each state is $\frac{1}{\sqrt{32}} \approx 0.18$ after this step. Oracle function only inverts the marked state $|w\rangle = |11111\rangle$ and keeps the other states unchanged. The phase flip method is used to invert the marked state. The amplitude of marked state $|w\rangle = |11111\rangle$ is inverted to $-\frac{1}{\sqrt{32}} \approx -0.18$. The combination of the Hadamard gate and CCCCZ gate is deployed to construct the

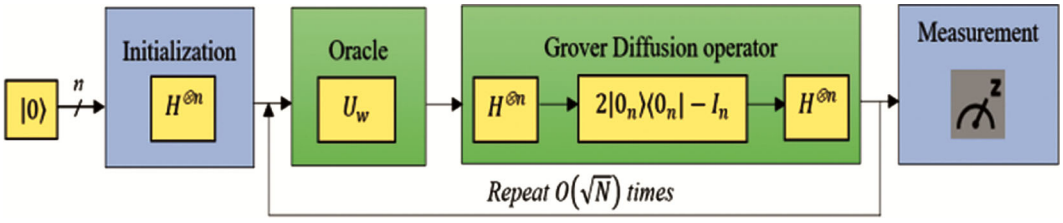

Fig. 5 — Schematic circuit for Grover's search algorithm for states $N = 2^n$. Oracle (U_w)and Grover diffusion operator is used with $O(\sqrt{N})$ iterations.

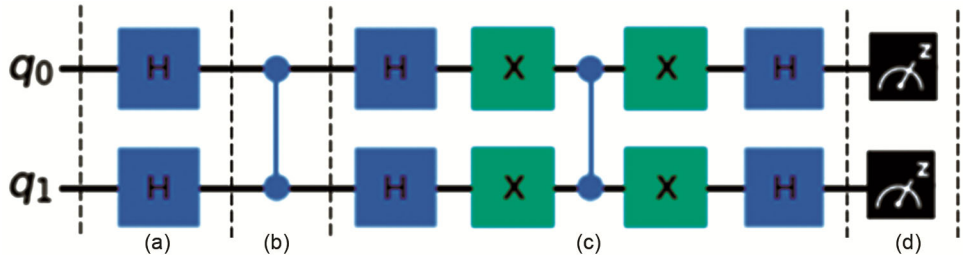

Fig. 6 — Quantum realization of 2-qubit Grover'salgorithm for finding $|w\rangle = |11\rangle$, (a) Initialization using Hadamard gate to put the qubits in superposition, (b) Controlled-Z (CZ) gate symbolizing an oracle to reflect the marked state $|11\rangle$, (c) Diffusion operator reflects the marked state again and amplifies it, (d) Measurement to detect the marked state $|11\rangle$.

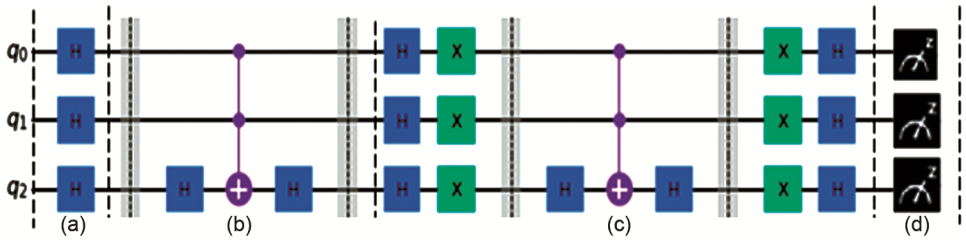

Fig. 7 — Quantum realization of 3-qubit Grover's algorithm for finding $|w\rangle = |111\rangle$, (a) Initialization using Hadamard gate to put the qubits in superposition, (b) Double controlled-Z (CCZ) gate symbolizing an oracle to reflect the marked state $|111\rangle$ where $Z = HXH$, (c) Diffusion operator reflects the marked state again and amplifies it, (d) Measurement to detect the marked state $|111\rangle$ in 2 iterations.

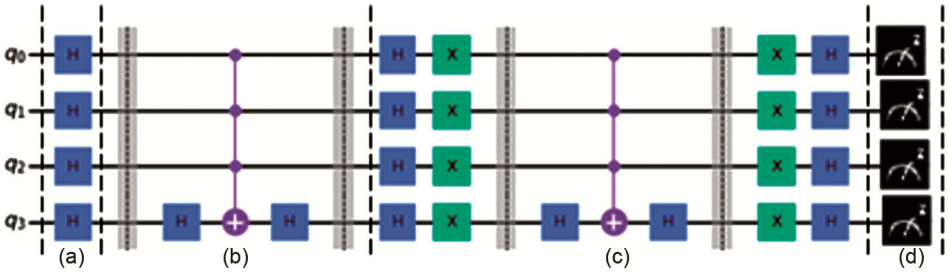

Fig. 8 — Quantum realization of 4-qubit Grover's algorithm for finding $|w\rangle = |1111\rangle$, (a) Initialization using Hadamard gate to put the qubits in superposition, (b) Triple controlled-Z (CCCZ) gate symbolizing an oracle to reflect the marked state $|1111\rangle$ where $Z = HXH$, (c) Diffusion operator reflects the marked sate $|1111\rangle$ and amplifies it. (d) Measurement to detect the marked state $|1111\rangle$ in 3 iterations.

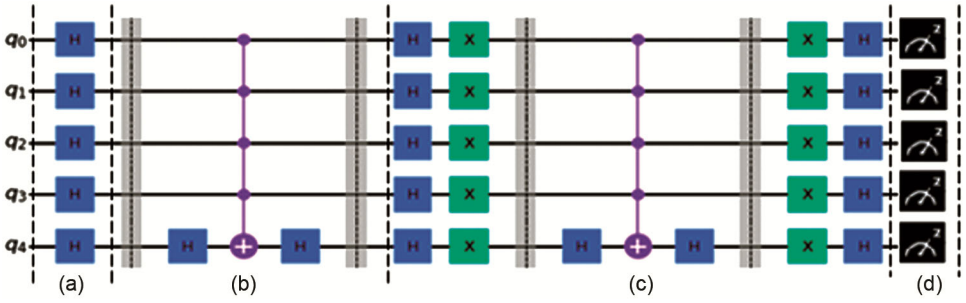

Fig. 9 — Quantum realization of 5-qubit Grover's algorithm for finding $|w\rangle = |11111\rangle$,(a)Initialization using Hadamard gate to put the qubits in superposition, (b) CCCCZ gate symbolizing an oracle to reflect the marked state $|11111\rangle$, where $Z = HXH$, (c) Diffusion operator reflects the marked sate $|11111\rangle$ and amplify it. (d) Measurement to detect the marked state $|11111\rangle$ in 4 iterations.

oracle as shown in Fig. 9(b). The amplification step inverts the amplitude of the marked state $|w\rangle = |11111\rangle$ about the average of the amplitudes by applying Grover's diffusion operator. The amplitude of the marked state is increased, whereas the amplitude of the unmarked states is decreased. Grover's diffusion operator is constructed using a combination of Hadamard, Pauli-X (NOT),and CCCCZ gates, as shown in Fig. 9(c).

The average amplitude is given by (11) as

$$\alpha_{avg} = \frac{31*0.18+(-0.18)}{32} \approx 0.17 \qquad \ldots(11)$$

The difference between the average amplitude (α_{avg}) and amplitude of the marked state $|w\rangle = |11111\rangle$, $\alpha_{|11111\rangle}$ is given by (12) as

$$d_{|11111\rangle} = \alpha_{avg} - (-0.18) = 0.35 \quad \ldots(12)$$

The inversion about the average amplitude results in increased amplitude of the marked state $|w\rangle = |11111\rangle$ given by (13) as

$$\alpha_{|11111\rangle} = \alpha_{avg} + d_{|11111\rangle} = 0.52 \quad \ldots(13)$$

The amplitude of each unmarked state is decreased and calculated as 0.16 using the same method. Finally, measurement gates shown in Fig. 9(d) are applied at the end of the quantum circuit to detect the marked state $|w\rangle = |11111\rangle$. The marked state $|w\rangle = |11111\rangle$ with better accuracy is obtained only with four iterations.

3.2 Quantum Gates Used in Oracle Formation

The controlled Z (CZ) and multi-controlled Z ($CCZ, CCCZ, CCCCZ$) are major gates involved in the construction of oracles, as shown in Tables 1-4. Pauli-Z gate is equivalent to the combination of Hadamard and Pauli-X gate given by (14) as

$$Z = HXH \quad \ldots(14)$$

CZ gate used in the construction of oracle and diffusion operator in 2-qubit implementation is

Table 1 — Accuracy results for Grover's algorithm implementations[3]

Implementation level	*Accuracy*
2-qubit	74.05%
3-qubit	59.69%
4-qubit	6.62%

Table 2 — Experimental results of Grover's algorithm implementations from 2 to 5 qubits

Grover's Algorithm	*No of gates*	*Depth of circuit*	*Number of Iterations*	*Simulator*		*Physical device(5-qubit)*	
				Accuracy (%)	Execution Time (s)	Accuracy (%)	Execution Time (s)
2-qubit	14	8	1	100	0.51	88.965	12.9
3-qubit	24	12	1	77.40	0.78	28.906	13.1
	42	22	2	94.60	0.91	30.505	13.2
	30	12	1	47.80	1.07	5.737	13.4
4-qubit	52	22	2	91.10	1.25	6.099	14.2
	74	32	3	96.20	1.60	6.251	14.2
	36	12	1	26	1.18	3.149	14.6
5-qubit	62	22	2	59.90	1.45	3.191	14.7
	88	32	3	89.80	1.84	3.198	15.9
	114	42	4	99.99	2.03	3.357	17.2

Table 3 — Noise parameters with their description[33]

Noise parameters	*Description*
Rotation error (r)	Rotation error arises either due to bit flip or phase flip, and both the operations with probability α. Kraus operators for bit flip, phase flip, and both are $\{\sqrt{1-\alpha}I, \sqrt{\alpha}\sigma_x\}$,$\{\sqrt{1-\alpha}I, \sqrt{\alpha}\sigma_y\}$ and$\{\sqrt{1-\alpha}I, \sqrt{\alpha}\sigma_z\}$respectively[34].
Decay (g)	The decay of a quantum system damages the quantum signal because of its impact on every qubit. The Kraus operators for decaying of quantum state with respect to the thermal state are $\left\{\sqrt{p}\begin{pmatrix}1 & 0\\ 0 & \sqrt{g}\end{pmatrix}, \sqrt{p}\begin{pmatrix}0 & \sqrt{1-g}\\ 0 & 0\end{pmatrix}, \sqrt{1-p}\begin{pmatrix}\sqrt{g} & 0\\ 0 & 1\end{pmatrix}, \sqrt{1-p}\begin{pmatrix}0 & 0\\ \sqrt{1-g} & 0\end{pmatrix}\right\}$, where *p* is the thermal factor, and *g* is the decay factor[33].
Decoherence (f)	Decoherence error arises due to the deterioration of quantum information present inside a quantum system when coupled with the environment. The Kraus operators for decoherence is $\left\{\sqrt{\frac{1+f}{2}}I, \sqrt{\frac{1+f}{2}}\sigma_z\right\}$, where *f* is the decoherence factor[33].
Depolarization (d)	Depolarization introduces errors generated by the quantum channel in a quantum communication link. Kraus operators for the depolarization channel is $\left\{\sqrt{1-\alpha}I, \sqrt{\frac{\alpha}{3}}\sigma_x, \sqrt{\frac{\alpha}{3}}\sigma_y, \sqrt{\frac{\alpha}{3}}\sigma_z\right\}$ where $\sigma_x, \sigma_y, \sigma_z$ are the computational basis, and *I* is the identity matrix[35].
Thermal (p)	The quantum information inside a quantum system degrades because of the thermal variations in an open quantum system.

Table 4 — Study of noise impact on accuracy and execution speed using QSIM

Grover's Algorithm (No of qubits)	*Marked states*	*Accuracy (%)*		*Execution Time (s)*	
		Without noise	With noise	Without noise	With noise
2	$\|11\rangle$	100	40	8	12
3	$\|111\rangle$	94.5	11	10	18
4	$\|1111\rangle$	96.13	6.5	13	24
5	$\|11111\rangle$	99	3.5	23	43

realized by using Hadamard and C-NOT gate together using (15) as

$$CZ = HCXH \quad ...(15)$$

3-, 4-, and 5-qubit implementations require $CCZ, CCCZ, CCCCZ$ gates, respectively, for oracle construction and diffusion operator formation. These gates are developed by using the combination of Hadamard and multi-controlled NOT gates given by (16)-(18) as

$$CCZ = HCCXH \quad ...(16)$$

$$CCCZ = HCCCXH \quad ...(17)$$

$$CCCCZ = HCCCCXH \quad ...(18)$$

The action of these multi-controlled Z gates is such that when all the controls are $|1\rangle$, target flips.

4 Experimental Evaluation

The experiments are performed on the quantum computer based on superconducting qubits technology. Various quantum computers and quantum simulators are publicly available on the cloud[29]. Grover's algorithm for 2-, 3-, 4-, and 5-qubit is implemented on the 32-qubit simulator back-end[16] using Qiskit[31] to compute the theoretical accuracy. Qiskit[31] software development kit contains quantum circuit simulators and real-time quantum processor back-ends for processing information encoded in qubits. All implementations of Grover's algorithm are realized on real-time quantum processor backend[17], which can be used for up to 16 qubits to check the physical accuracy of the algorithm. There is a maximum of 8192 shots available to execute a circuit. Therefore, the same number of shots were utilized for searching every state. In addition to the implementation of Grover's algorithm up to 5-qubit, the variations in the accuracy and execution time caused by noise present in noisy intermediate-scale quantum computers (NISQ) have been investigated. Various noise parameters are taken into consideration for the evaluation.

4.1 Number of Qubits, Gates, and Iterations

It is observed that by increasing the number of qubits from 2 to 5-qubit, the gate count increases. The number of gates increased from 14 to 114 for 2 to 5-qubit implementations, as shown in Table 2. The correct marked state with better accuracy will be detected when the oracle and diffusion operator is repeated several times. This repetition of the oracle and diffusion operator together is called iteration[12]. All the possible iterations are taken up to $round\left(\frac{\pi}{4}\sqrt{N}\right)$,which means one iteration for 2-qubit, up to 2 iterations for 3-qubit, up to 3 iterations for 4-qubit, and up to 4 iterations for 5-qubit implementations. It is observed that in order to obtain the correct marked state with better accuracy $round\left(\frac{\pi}{4}\sqrt{N}\right)$ number of iterations are required, which means four iterations are required for 5-qubit implementations of Grover's algorithm.

4.2 Depth of the Circuit

The depth of the circuit is the extensive route starting from the input (initialization) and ending at the output (measurement)[30]. With increasing the number of qubits, the depth of the circuit is also increased. As the number of qubits are increased from 2-to 5-qubit, the depth of the circuit increases from to 8 to 42. The depth of circuits computed for all the possible iterations is listed in Table 2.

4.3 Theoretical accuracy

The accuracy or algorithm success probability (ASP) of Grover's algorithm is the probability of detecting the correct marked state. The ASP after the single iteration of Grover's algorithm can be calculated by $t.\left[\left(\frac{N-2t}{N}+\frac{2(N-t)}{N}\right)\frac{1}{\sqrt{N}}\right]^2$ for single marked solution (t=1) [30]. Theoretically, the accuracy of Grover's algorithm for 2-qubit is 100 % with one iteration; for 3-qubit, the accuracy is 94.60 % with two iterations; for 4-qubit, accuracy is 96.20 % with three iterations, and for 5-qubit accuracy is 99.99 % with four iterations as shown inTable 2. As the number of iterations for each qubit implementation increases up to $round\left(\frac{\pi}{4}\sqrt{N}\right)$as listed in Table 2, the theoretical accuracy of the algorithm gets better. It can be observed from Table 2 that the theoretical accuracy is above 94% for all these implementations of Grover's algorithm.

5 Physical Accuracy and Execution Time

The comparison between the physical accuracy of the earlier Grover's algorithm implementations for 2-, 3-, and 4-qubit are illustrated in Table 1[3]. This experiment was conducted with 8192 shots. It is seen that the accuracy of Grover's algorithm decreases as the number of qubits is increased. The accuracy of Grover's algorithm for 3- and 4-qubit implementations is decreased by 19.39 % and 91.06% compared to the accuracy of 2-qubit implementation[3].

In this study, all the implementations up to 5-qubit are performed on the physical device back-ends also. It could be observed from the results shown in Table 2 that the physical accuracy of the algorithm decreases as the number of qubits increases from 2 to 5 by 96.22 %, and the execution time increases by 33.33 % for physical device. Table 2 also depicts a huge difference between the theoretical and physical accuracy of the algorithm implementations. In the case of 5-qubit implementation with four iterations, the physical accuracy of the algorithm decreases by 96.64 % compared to theoretical accuracy.

From Table 2, it can be observed that for 2-qubit implementation, the physical accuracy of the algorithm decreases by 11.04 % compared to theoretical accuracy. For 3-qubit implementation, the physical accuracy of the algorithm decreases by 62.66 % with a single iteration and 67.75 % with two iterations compared to the theoretical accuracy of the algorithm. In the case of 4-qubit implementation, the degradations of physical accuracy by 88.01 % for one iteration, 93.30 % for two iterations, and 93.50 % for three iterations have been observed.

Similarly, the degradation of 87.88% for one iteration, 94.67% for two iterations, 96.43% for three iterations, and 96.64% for four iterations have been observed in the physical accuracy for 5-qubit implementation. The degradation in the theoretical accuracy from 2 to 3 qubits is 22.6 %, from 3 to 4 qubits is 38.24 %, and from 4 to 5 qubits is 45.60 %. In contrast, the physical accuracy degradation from 2 to 3 qubits is 67.51%, from 3 to 4 qubits is 78.89 %, and from 4 to 5 qubits is 45.04 % for a single iteration. For two iterations, theoretical accuracy degradation from 3 to 4 qubits is 3.70 % and from 4 to 5 qubits is 34.25%, whereas physical accuracy degradation from 3 to 4 qubits is 80 % and from 4 to 5 qubits is 47.68 %. Similarly, for three iterations, the degradation in theoretical and physical accuracy from 4 to 5 qubits is 6.65 % and 48.83 %, respectively.

6 Noise Analysis

Noise is significantly affecting the accuracy and speed of existing quantum bits. The major difference between theoretical and physical accuracies of quantum devices is due to noise only. Noisy interactions between entangled qubits and material impurities may cause internal noise in quantum circuits/systems, whereas stray fields and control electronics result in external noise. The ability to reduce noise is a major focus in developing quantum computers. The investigation of noise impact in the implementation of quantum circuits and systems is becoming of at most importance. In conventional quantum computing, the quantum states are expressed in terms of basis states, generally as linear combinations. However, there are use cases where it is impossible to represent quantum states as linear combinations of basis states. In these cases, the density matrix representation of quantum states becomes very useful. Simply put, the density matrix is an alternative way of expressing quantum states. In this paper, the QSIM[33] simulator has been utilized to compute the noise performance of Grover's algorithm. QSIM simulator utilizes the density matrix formalism to compute changes in the state of a qubit when gates are applied to it. The density matrix formalism permits the incorporation of environmental noises according to convenience. The designed circuits in this simulator can be implemented with or without noise. The accuracy and execution time for both with and without noise cases is experimentally evaluated. The number of iterations used in the experiment is $round\left(\frac{\pi}{4}\sqrt{N}\right)$. When the number of qubits in Grover's algorithm increases, the iterations also increase. The increase in iterations results in the increased depth of the circuit. This implies an increase in the number of gates in the circuit. The increased number of gates is one of the factors which increases the noise in the circuit. Table 3 depicts various noise parameters taken in this experiment, and Table 4 reveals the accuracy evaluation of Grover's algorithm up to 5-qubit on the QSIM simulator. The accuracy for 2-qubit implementation without noise when searching for marked state $|11\rangle$is decreased by60% compared to the same implementation with noise, as revealed in Fig. 10 (a). Also, for 3-qubit implementation without noise for marked state$|111\rangle$, the accuracy of Grover's algorithm is reduced by 88.35% compared to the same implementation with noise, as revealed in Fig. 10(b). In

the case of 4-qubit implementation of searching a marked state $|1111\rangle$ without noise, the accuracy of Grover's algorithm decreased by 93.23% compared to the same implementation with noise. Similarly, the accuracy for 5-qubit implementation for searching marked state $|11111\rangle$ without noise is reduced by 96.46% as compared to the same implementation with noise parameters. Grover's algorithm implementations take less time when no noise is considered, and the execution time increases when the noise is considered.

The execution time of a 2-qubit implementation without noise parameters is 50% higher compared to the same implementation with noise parameters. For a 3-qubit implementation without noise, the execution time is increased by 80% compared to the same implementation with noise parameters. Without considering the noise parameters for 4-qubit implementation, the execution time is increased by 84.6% compared to the same implementation with noise parameters. Similarly, 5-qubit implementation without noise, an increment of 86.95% is observed when compared to the same implementation after considering the noise parameters.

Table 5 depicts the decrease in the accuracy of Grover's algorithm for 2- and 3-qubit when noise is introduced in the system. The noise study reveals that thermal and depolarization errors are the smallest errors, rotation errors are the moderate errors, and decoherence and decay are the prominent errors. The accuracy of Grover's algorithm for 2-qubit and 3-qubit is decreased by 14.49% and 33.86%, respectively, as noise parameter values vary from the ideal value. Similarly, the decrease in the accuracy of Grover's algorithm for 4- and 5-qubit is also observed.

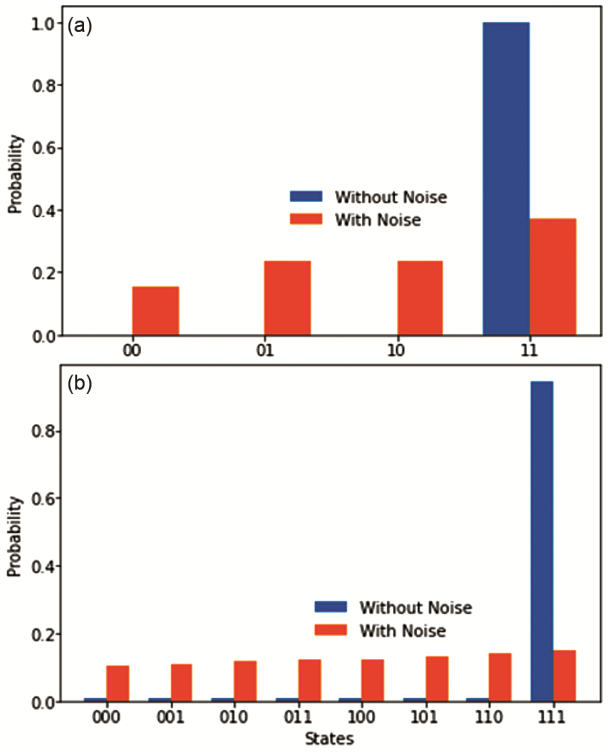

Fig. 10 — (a): Variation in the accuracy of 2- qubit implementation for searching $|11\rangle$ with and without noise, (b) Variation in the accuracy of 3- qubit implementation for searching $|111\rangle$ with and without noise.

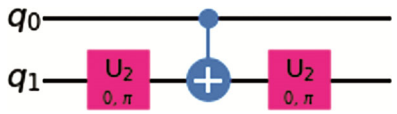

Fig. 11 — Decomposition of CZ gate. $U_2(0,\pi)$ is equivalent to the Hadamard gate.

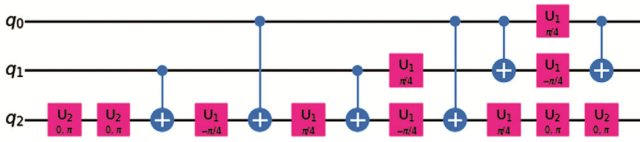

Fig. 12 — Decomposition of CCZ gate. CX, U_1, U_2 gates are used multiple times. Also, $U_1\left(\frac{\pi}{4}\right) = T$, $U_1\left(-\frac{\pi}{4}\right) = T^\dagger$ and $U_2(0,\pi) = H$.

Table 5 — Effect of various noises parameters on the accuracy of Grover's algorithm

Grover's Algorithm	*Marked states*	*Noise Parameters*					*Accuracy (%)*
		Rotation (r)	*Decay (g)*	*Decoherence (f)*	*Depolarization (d)*	*Thermal (p)*	
2-qubit	$\|11\rangle$	1	1	1	1	1	100
		0.998	0.99998	0.9998	0.98	0.98	95.98
		0.996	0.99996	0.9996	0.96	0.96	92.15
		0.994	0.99994	0.9994	0.94	0.94	85.51
3-qubit	$\|111\rangle$	1	1	1	1	1	94.50
		0.998	0.99998	0.9998	0.98	0.98	82.09
		0.996	0.99996	0.9996	0.96	0.96	71.56
		0.994	0.99994	0.9994	0.94	0.94	62.64

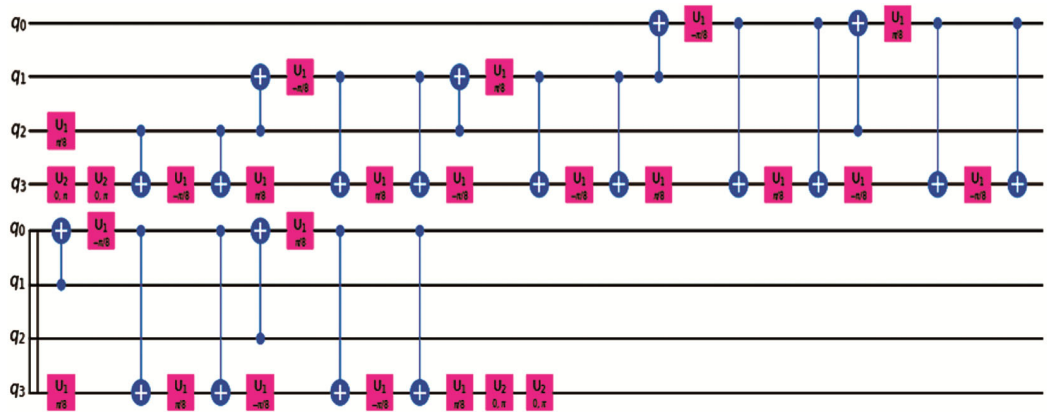

Fig. 13 — Decomposition of CCCZ gate. Like CCZ decomposition, CX, U_1, U_2 gates are used multiple times, but the rotation of U_1 is different, i.e., $\frac{\pi}{8}$. Here, $U_1\left(\frac{\pi}{8}\right) = z^{\frac{1}{8}}$, $U_1\left(-\frac{\pi}{8}\right) = z^{-\frac{1}{8}}$ and $U_2(0,\pi) = H$.

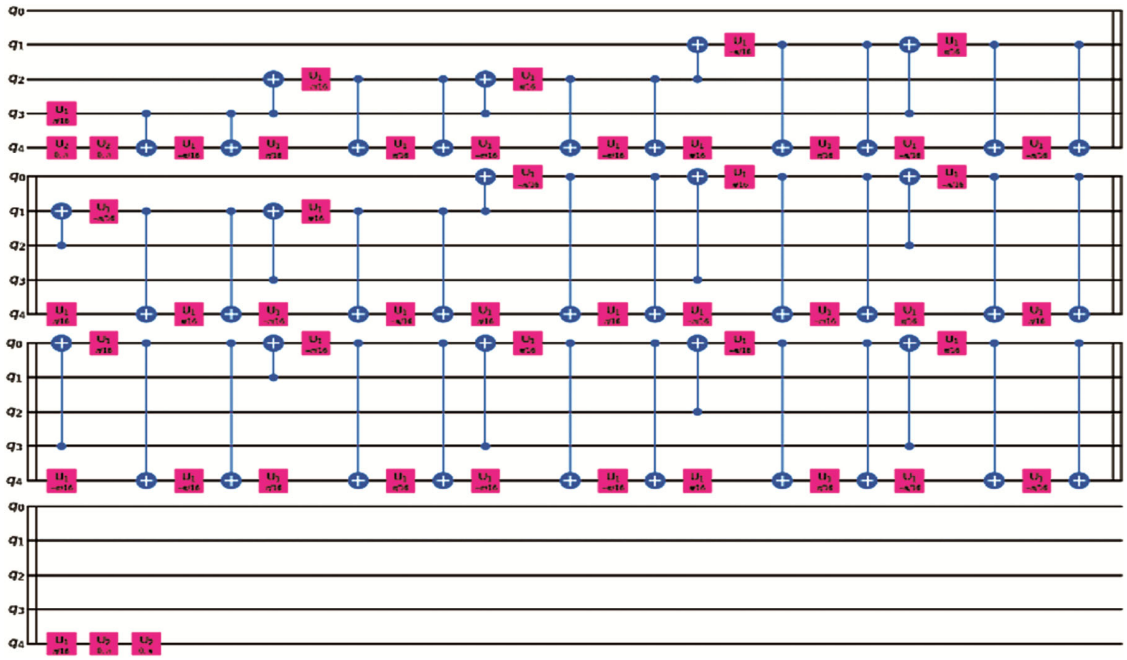

Fig. 14 — Decomposition of CCCCZ gate. CCCCZ decomposition also includes CX, U_1, U_2 gates where the rotation of $U_1 = \frac{\pi}{16}$. Here, $U_1\left(\frac{\pi}{16}\right) = z^{\frac{1}{16}}$, $U_1\left(-\frac{\pi}{16}\right) = z^{-\frac{1}{16}}$ and $U_2(0,\pi) = H$.

7 Conclusions

The accuracy and execution time assessment of Grover's algorithm up to 5-qubit is carried out. The experimental results explicitly prove that as the number of qubits increases, the physical accuracy of the algorithm decreases, and the execution time increases when a real-time quantum computer is used. There is a huge difference between the theoretical accuracy and the physical accuracy of Grover's algorithm with $round\left(\frac{\pi}{4}\sqrt{N}\right)$ iterations. The variation in the accuracy and execution time is because of noisy quantum systems. The experimental results also show a decline in the accuracy and a rise in the execution time when environmental noise is introduced. Different kinds of noises have a different impact on the accuracy of Grover's search algorithm. Thermal and depolarization errors are small, rotation errors are moderate while decay and decoherence errors are large. So, it could be concluded that Grover's quantum search algorithm is good only for searching in small databases, whereas its accuracy degrades significantly because of the noise when the number of qubits increases. Thus, optimization of Grover's algorithm is required in order to improve the accuracy for higher counts of qubits.

Declarations

Conflict of interest: Authors declare that there is no conflict of interest.

Appendix

The multi-controlled-Z gates (CCZ, CCCZ, and CCCCZ) are not present in the QISKIT. So, these gates have been realized using CX and Unitary gates (U_1, U_2) with their different rotations. In this section, the decomposition of the CZ and other multi-controlled-Z gates used in the implementation of Grover's algorithm has been described. In this experiment, CZ, CCZ, CCCZ, and CCCCZ have been considered as a single gate. The decompositions in Figs. 11-14 have been provided to give the idea about implementations of CZ and multi-controlled-Z gates.

References

1 Ladd T D, Jelezko F, Laflamme R, Nakamura Y, Monroe C & O'Brien J L, *Nature*, 464 (2010) 45.
2 Saini S, Khosla P, Kaur M & Singh G, *Int J Theor Phys*, 59 (2020) 4013.
3 Mandviwalla A, Ohshiro K, *et al.*, *International Conference on Big Data (Big Data),* IEEE, USA, (2018) 2531.
4 Singh G, Kaur M, Singh M & Kumar Y, *Indian J Pure Appl Phys*, 60 (2022) 407.
5 Szalay A S, Gray J & Vanden Berg J, *Proc SPIE,* 4836 (2002) 33.
6 Wolf R de, *Ethics Info Technol J,* 19 (2017) 271.
7 Harrow A W, Hassidim A & Lloyd S, *Phy Rev Lett,* 103 (2009) 150502.
8 Shor P W, *Proc 35th Annual Symposium on Foundations of Computer Science,* IEEE, USA, (1994) 124.
9 Grover L K, *Proc 28th Annual ACM Symposium on the Theory of Computation,* ACM Press, USA, (1996) 212.
10 Rieffel E & Polak W, *ACM Comput Surv,* 32 (2000) 300.
11 Nagy M & Akl S G, *Int J Parallel Emergent Distrib Syst,* 21 (2006) 1.
12 Nielsen M A & Chuang I L, *Quantum Computation and Quantum Information*, (Cambridge University Press, UK), 10th Edn, 2010.
13 Acampora G *et al.*, *Inf Fusion,* 89 (2023) 16.
14 Kumar T, Kumar D, Singh G, *Indian J Pure Appl Phys,* 60 (2022) 644.
15 Kumar T *et al*., *Chinese J Phys*, 83 (2023) 277.
16 IBM Inc, Ibmq_qasm_simulator.http://quantum-computing.ibm.com/?system=ibmq_qasm_simulator.
17 IBM Inc., Ibmq_santiago. *https://quantum-computing. ibm.com/ ?system=ibmq_santiago*.
18 Coles P J, Eidenbenz S, Pakin S, Adedoyin A, Ambrosiano J, *et al.*, *arXiv preprint arXiv:1804.03719*, (2018).
19 Hu W, *Natural Science,* 10 (2018) 45.
20 Figgatt C, Maslov D, Landsman K, *et al., Nature Commun J,* 8 (2017)1918.
21 Stromberg P & Karlsson V B, *4-qubit Grover's algorithm implemented for the ibmqx5 architecture,* Degree project, KTH royal institute of technology, Sweden, 2018.
22 Simon D R, *SIAM J Comput,* 26 (1997) 1474.
23 Jozsa R, arXiv *preprint quant-ph/9901021*, (1999).
24 Lloyd S, Mohseni M & Rebentrost R, arXiv*:1307.0411v2 [quant-ph], (*2013).
25 Nahimovs N & Rivošs A, *Sci Papers Univ Latvia*, 756 (2010) 221.
26 Kwiat P G *et al., J Mod Opt,* 47 (2000) 257.
27 Zalka C, *Phys Rev A,* 60 (1999) 2746.
28 IBM Inc, Quantum information science kit-Grover'sAlgorithm.https://qiskit.org/textbook/ch-algorithms/grover.html.
29 IBM Inc, IBM quantum experience.https:// quantumexperience.ng.bluemix.net/qx/experience.
30 Mitarai K, Negoro M, Kitagawa M & Fujii K, *Phys Rev A,* 98 (2018) 032309.
31 IBM Inc, Quantum information science kit. https://qiskit.org/aqua.
32 Chen Y T, Farquhar C &Parrish R M, *NPJ Quantum Inf,* 7 (2021) 61.
33 Chaudhary *et al., arXiv:1908.05154 [quant-ph],* (2019).
34 Gawron P, *et al., Int J Appl Math Comput Sci,* 22 (2012) 493–499.
35 Amaral G C *et al*., *Quantum Inf Process,* 18 (2019) 342.